



Multi-scale evaluation of high-resolution multi-sensor blended global precipitation products over the Yangtze River



Zhe Li^a, Dawen Yang^{a,*}, Yang Hong^{b,c}

^a Department of Hydraulic Engineering, Tsinghua University, Beijing 100084, China

^b Hydrometeorology and Remote Sensing Lab, Department of Civil Engineering and Environmental Science, University of Oklahoma, Norman, OK 73072, United States

^c Advanced Radar Research Center, National Weather Center, Suite 4160, Norman, OK 73072, United States

ARTICLE INFO

Article history:

Received 23 March 2013

Received in revised form 20 June 2013

Accepted 16 July 2013

Available online 25 July 2013

This manuscript was handled by Geoff Syme, Editor-in-Chief, with the assistance of Bellie Sivakumar, Associate Editor

Keywords:

Satellite precipitation
Statistical evaluation
Error characteristics
Yangtze River

SUMMARY

In the present study, four high-resolution multi-sensor blended precipitation products, TRMM Multisatellite Precipitation Analysis (TMPA) research product (3B42 V7) and near real-time product (3B42 RT), Climate Prediction Center MORPHing technique (CMORPH) and Precipitation Estimation from Remotely Sensed Information using Artificial Neural Networks (PERSIANN), are evaluated over the Yangtze River basin from April 2008 to March 2012 using the gauge data. This regional evaluation is performed at temporal scales ranging from annual to daily, based on a number of diagnostic statistics. Gauge adjustment greatly reduces the bias in 3B42 V7, a post real-time research product. Additionally, it helps the product maintain a stable skill level in winter. When additional indicators such as spatial correlation, Root Mean Square Error (RMSE), and Probability of Detection (POD) are considered, 3B42 V7 is not always superior to other products (especially CMORPH) at the daily scale. Among the near real-time datasets, 3B42 RT overestimates annual rainfall over the basin; CMORPH and PERSIANN underestimate it. In particular, the upper Yangtze always suffers from positive bias ($>1 \text{ mm day}^{-1}$) in the 3B42 RT dataset and negative bias (-0.2 to -1 mm day^{-1}) in the CMORPH dataset. When seasonal scales are considered, CMORPH exhibits negative bias, mainly introduced during cold periods. The correlation between CMORPH and gauge data is the highest. On the contrary, the correlation between 3B42 RT and gauge data is more scattered; statistically, this results in lower bias. Finally, investigation of the probability distribution functions (PDFs) suggests that 3B42 V7 and 3B42 RT are consistently better at retrieving the PDFs in high-intensity events. Overall, this study provides useful information about the error characteristics associated with the four mainstream satellite precipitation products and their implications regarding hydrological applications over the Yangtze River basin.

© 2013 Elsevier B.V. All rights reserved.

1. Introduction

Precipitation is the key forcing factor that provides essential input information for estimating land surface hydrological fluxes and states (Nijssen and Lettenmaier, 2004), and the response of hydrological system is always significantly affected by the intensity, duration, area coverage and spatial pattern of precipitation (Heistermann and Kneis, 2011; Sorooshian et al., 2011), especially for those natural hazards linked with precipitation extremes, such as floods, droughts, and landslides (Hong et al., 2006; Aragão et al., 2007; Wu et al., 2012).

Despite its crucial importance in many hydrological and meteorological applications, accurate measurement of precipitation at

regional or global scale with fine resolution remains challenging due to its great heterogeneity across a variety of spatiotemporal scales. Traditionally, the most widely used rain gauges are distributed sparsely and unevenly, and they are always insufficient for precipitation monitoring in remote regions, ungauged basins, or areas with complex terrain (Huffman et al., 2001; Mishra and Coulibaly, 2009). Weather radar can monitor regional precipitation with relatively high resolution; however, it suffers from the problem of reduced data quality in complex terrain as a result of distorted electronic signals introduced by the surrounding environment (Tian et al., 2010; Zhang et al., 2011).

An alternative method relying on satellite-based precipitation retrieval algorithms to estimate large-scale precipitation dynamics has recently been developed. A series of multi-sensor blended global precipitation products are being released in a near real-time manner. These products have high spatiotemporal resolution (0.25° and 3 h or finer) and include PERSIANN (Sorooshian et al.,

* Corresponding author. Address: Room 312, New Hydraulic Engineering Building, Department of Hydraulic Engineering, Tsinghua University, Beijing 100084, China. Tel.: +86 10 62796976.

E-mail address: yangdw@tsinghua.edu.cn (D. Yang).

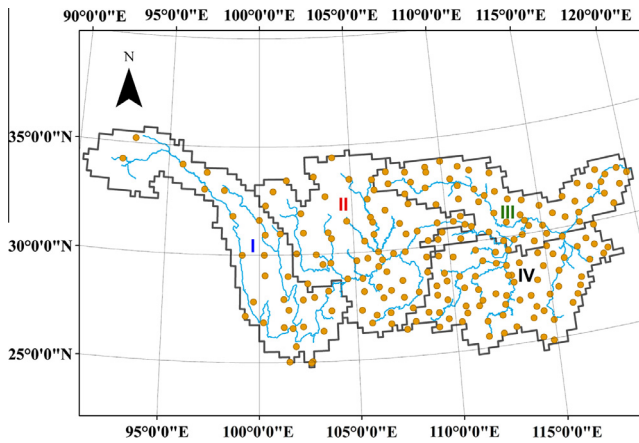


Fig. 1. Rain gauges distribution and sub-regions division of Yangtze River. (Region I: the west part of the upper Yangtze River; Region II: the east part of the upper Yangtze River; Region III: the north side of the lower Yangtze River; Region IV: the south side of the lower Yangtze River).

2000), CMORPH (Joyce et al., 2004), PERSIANN-CCS (Hong et al., 2004), NRL-Blend (Turk and Miller, 2005), TMPA (Huffman et al., 2007), and GSDMap (Kubota et al., 2007). In the near future, as a

result of the Global Precipitation Measurement (GPM) mission, the next generation of satellite-derived precipitation estimates will achieve a resolution of 4 km and 30 min (Sorooshian et al., 2011). Additionally, these GPM-era products will be able to get much more reliable precipitation information from space-borne sensors.

Due to the significant improvement of global satellite-based precipitation estimate techniques during the past decades, a great number of hydrological studies applying satellite precipitation products have made it into the literature. Recently the hydrological prediction community has recognized the opportunity these products offer to improve flood monitoring over medium to large river basins (Hossain and Lettenmaier, 2006). Other works have demonstrated that the continuing evolution of retrieval algorithms provides increasing potential for the use of these products in hydrological simulations (Su et al., 2008; Yong et al., 2012). Before these products can be used in hydrological applications, the errors associated with these products should be characterized so that the data can be used as effectively as possible (Turk et al., 2008). The performance of different satellite-based precipitation estimation products can also change as retrieval algorithms and data sources change (Ebert et al., 2007; Hirpa et al., 2010; Jiang et al., 2012). For the same product, performance can vary remarkably between regions, seasons and precipitation regimes (Ebert et al., 2007; Dinku et al., 2010). In addition, there is also a trade-off between the quality of the estimate and the spatiotemporal scale of the product

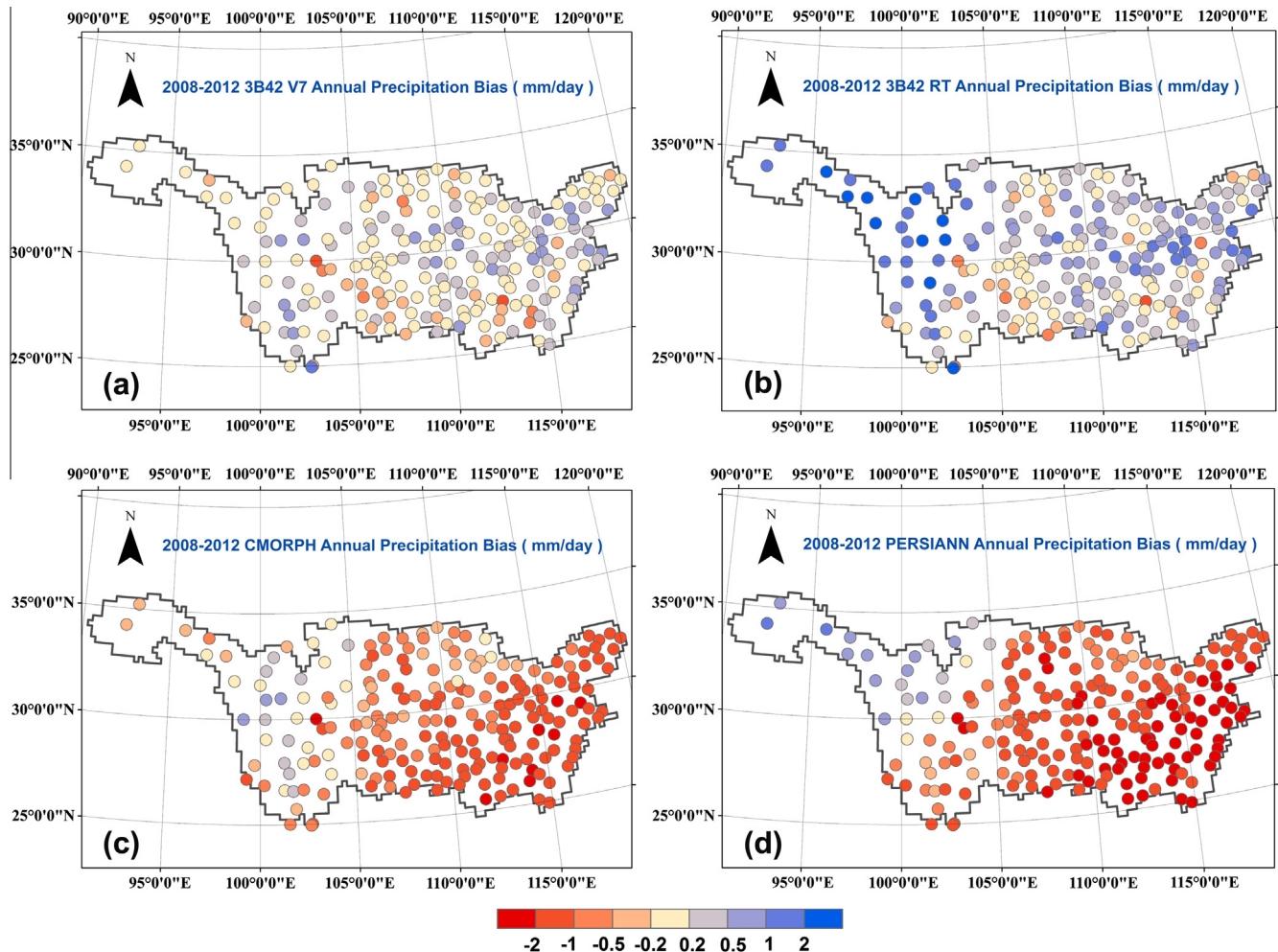


Fig. 2. Bias (mm day^{-1}) for annual mean precipitation between the satellite precipitation products of (a) 3B42 V7 and gauge; (b) 3B42 RT and gauge; (c) CMORPH and gauge; and (d) PERSIANN and gauge from Apr 2008 to Mar 2012.

Table 1

Statistics of annual precipitation for each year during 2008–2012, averaged over the whole Yangtze River.

		2008–2009	2009–2010	2010–2011	2011–2012
Gauge	Mean (mm)	1131	1073	1220	1050
	3B42 V7				
3B42 V7	Mean (mm)	1201	1123	1224	1071
	RB (%)	6.24	4.72	0.27	1.99
	RMSE (mm)	174.13	170.74	177.89	159.65
	CORR	0.89	0.88	0.92	0.91
3B42 RT	Mean (mm)	1372	1190	1407	1247
	RB (%)	21.39	10.97	15.30	18.88
	RMSE (mm)	378.26	338.00	344.55	335.00
	CORR	0.65	0.59	0.79	0.74
CMORPH	Mean (mm)	817	680	873	683
	RB (%)	–27.81	–36.65	–28.44	–34.93
	RMSE (mm)	406.24	491.27	452.00	454.59
	CORR	0.65	0.46	0.77	0.69
PERSIANN	Mean (mm)	510	598	703	555
	RB (%)	–54.92	–44.22	–42.36	–47.09
	RMSE (mm)	704.46	629.61	639.47	609.17
	CORR	0.19	–0.17	0.54	0.30

(Sorooshian et al., 2011). Thus, it is necessary to know the quality of satellite-based precipitation estimates via a comprehensive evaluation. The properties of the errors dictate how the data can be used appropriately in hydrological applications. Additionally, knowledge of the error properties is helpful in future development of retrieval algorithms. Motivated by this twofold aim, there have been many efforts to evaluate and intercompare available satellite-based precipitation products at global, regional or basin scales (Ebert et al., 2007; Tian et al., 2007; Turk et al., 2008; Gourley et al., 2010; and many others).

In China, several validation studies of satellite precipitation products have been conducted recently at national or regional scales. Zhou et al. (2008) compared the diurnal cycle of precipitation estimated by PERSIANN and TMPA 3B42 with gauge observations over China. Yin et al. (2008) compared satellite products with gauge data, and found that TMPA 3B42 consistently overestimated monthly rainfall over the Tibetan Plateau. Shen et al. (2010) analyzed the performance of six of the most popular high-resolution products over the Chinese mainland based on hourly gauge observations for a 3-year period from 2005 to 2007. Yong et al. (2012) and Jiang et al. (2012) mainly focused on basin scale evaluation of satellite precipitation products, and, in so doing, demonstrated the promises and problems in applying these datasets to watershed hydrological simulations. However, since all these datasets are still undergoing updates, long-term systematic evaluation of these datasets over different regions in China is difficult, especially where complicated precipitation regimes exist. This is a problem for medium to large river basins such as the Yangtze River.

The Yangtze River, the largest river in China, is known to be extremely susceptible to frequent floods due to heavy rainfall events that usually occur between April and September (Heike et al., 2012). The subtropical monsoon and the effects of complex terrains generate complicated precipitation regimes over the whole Yangtze, so near real-time monitoring of precipitation over this region is essential for developing a good hydrological prediction and warning system (Sohn et al., 2012). In this paper we focus on an evaluation and intercomparison of TMPA 3B42 V7 (hereinafter referred to as 3B42 V7), TMPA 3B42 RT V7 (hereinafter referred to as 3B42 RT), CMORPH and PERSIANN products with the same resolution (0.25° and 3 h) over the Yangtze, and try to quantify and document the error characteristics associated with these different satellite-based precipitation estimates. This will serve as an initial step for the establishment of a distributed hydrological prediction

system over the Yangtze River. We extend previous evaluation work related to this region (Shen et al., 2010; Gu et al., 2010; Li et al., 2012; Jiang et al., 2012) in three aspects. First, we chose a recent four years study period (April, 2008 to March, 2012) to provide up-to-date insight into the skill of the latest satellite-based products. The TMPA products will integrate new sensors and their retrieval algorithms will undergo several updates during the course of routine product development (Yong et al., 2012). Here we adopt the latest released version 7 of TMPA products (3B42 V7 and 3B42 RT), and evaluate it over the Yangtze River. Second, we intercompare a number of high-resolution precipitation products at different temporal scales using multiple statistical metrics. We believe this kind of comprehensive evaluation work will determine the appropriate satellite-based precipitation product for use over the Yangtze in hydrological applications. One thing to be noted here is that the diurnal precipitation cycle has been discussed extensively in previous studies (Zhou et al., 2008; Shen et al., 2010). Here, we leave this critical issue for a future study because our access to regional hourly gauge data is limited. Finally, we determine the skill of each precipitation estimate over the entire Yangtze, because this overview provides more complete information about the regional variations in the error characteristics of each product while further benefitting our understanding of rainfall-runoff simulations in the region.

The remaining parts of this paper are organized as follows: the gauge and satellite precipitation datasets are addressed in Section 2, including how the datasets were post-processed to allow for intercomparison. Section 3 discusses the multi-scale evaluation results according to a number of statistical metrics that emphasize different aspects of validation and the implications of each to hydrological prediction. Finally, Section 4 summarizes conclusions from and discussion of these evaluation results.

2. Data and methodology

2.1. Satellite-based precipitation products

The satellite products to be evaluated here include four sets of popular high-resolution multi-sensor blended precipitation products: 3B42 V7, 3B42 RT, CMORPH and PERSIANN. All these products are generated by combining information from both passive microwave (PMW) observations and infrared (IR) observations.

3B42 RT and PERSIANN utilize PMW-calibrated IR techniques, which assume the PMW estimates are accurate enough to represent the ground rainfall. PERSIANN offers precipitation estimates every 3 h on a 0.25° latitude/longitude grid with quasi-global coverage (60°S–60°N) since March 2000. 3B42 RT has been generated since 1998 with the same temporal and spatial resolution as PERSIANN; its spatial coverage varies slightly (50°S–50°N). CMORPH uses a different technique called the Lagrangian interpolation approach to combine PMW and IR measurements, where PMW estimates are propagated by IR-derived advection vectors. CMORPH products used in this study are also generated on 0.25° spatial grids every 3 h with coverage from 60°S to 60°N.

All three products mentioned above are generated solely from satellite observations, but 3B42 V7 further takes into account ground gauge information to remove the bias of satellite retrievals. The latest Version 7 products ingest PMW observations from the Special Sensor Microwave Imager/Sounder (SSMIS) carried aboard the Defense Meteorological Satellite Program (DMSP) and the new Global Precipitation Climatology Centre (GPCC) “full” gauge analysis, when available (Huffman et al., 2011). Certainly 3B42 V7 contains information that is in some sense shared with 3B42 RT; we compare them here to see the impacts of gauge observations on the error characteristics of satellite precipitation products.

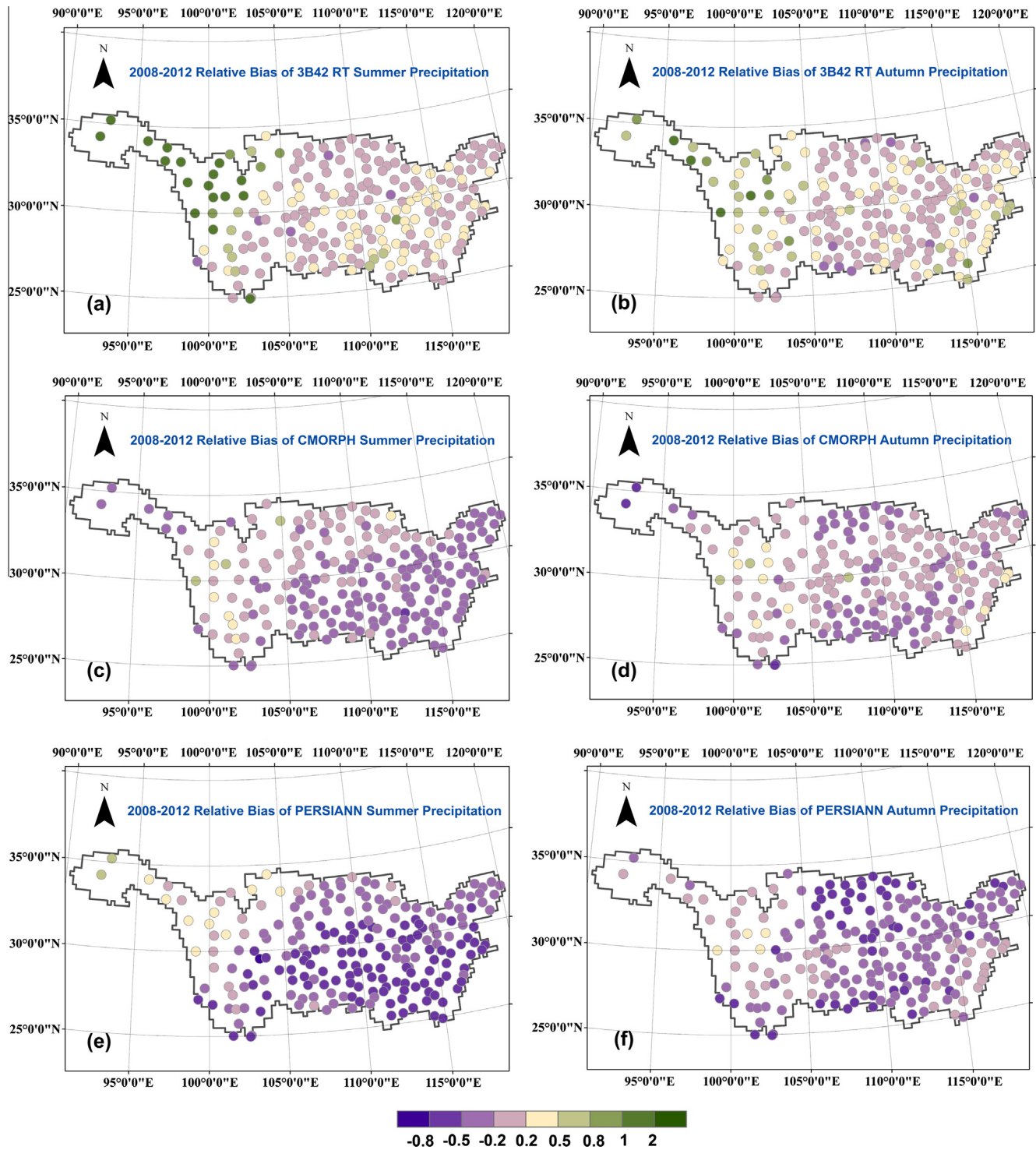


Fig. 3. Relative bias of seasonal precipitation for the warm period: summer (left) and autumn (right), and from top to bottom are: 3B42 RT, CMORPH, and PERSIANN.

2.2. The gauge data

Gauge observations play a critical role in the quantitative evaluation of satellite-based precipitation products. Here we adopted the new Version 3.0 of China Daily Ground Climate Dataset (CDGCD-V3) produced routinely by the National Meteorological Information Center (NMIC) of the China Meteorological Administration (CMA). This latest released CDGCD-V3 consists of 824 gauges in China to generate nation-wide daily climate

observations, including air pressure, air temperature, relative humidity, precipitation, evaporation, wind speed and wind direction, sunshine duration, and 0 cm ground temperature. In this paper, we only adopt the daily precipitation records from each gauge for our evaluation work.

The CDGCD-V3 is performed with a strict quality control procedure, and it is claimed there's a substantial improvement in the accuracy and completeness of observation compared with previous versions of CDGCD (China Meteorological Administration, 2012).

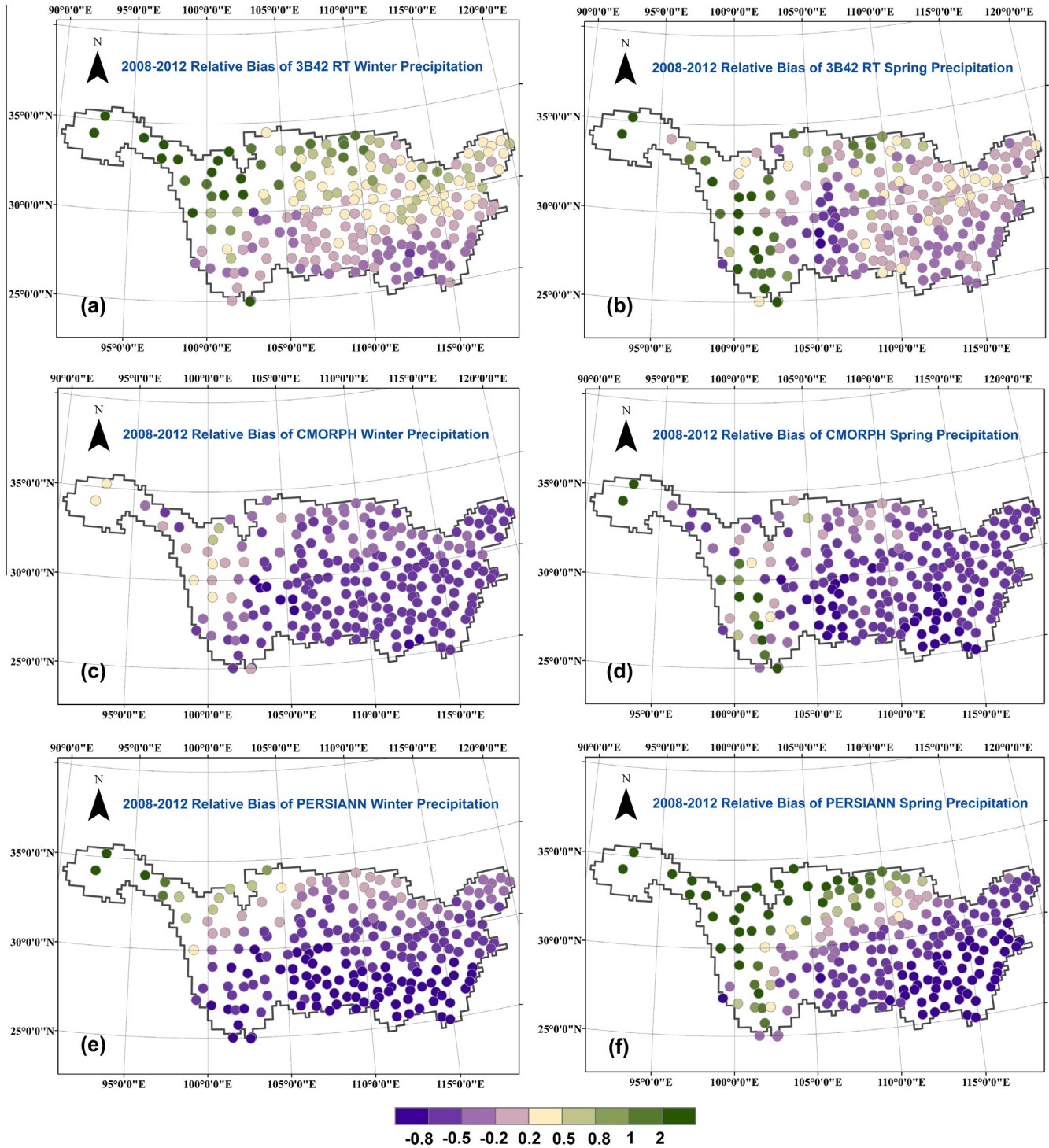


Fig. 4. The same as Fig. 3 but for the cold period: winter (left) and spring (right).

This Version 3.0 data incorporates manual checking and correction for error or uncertain observations, and it guarantee the accuracy of data approximates as high as 100%.

2.3. Evaluation method

First, we selected daily precipitation records from 215 gauges that located within the Yangtze River (Fig. 1). Although the spatial resolution of the global satellite products (0.25°) is not perfectly matched with the gauge data (point measurement), in order to

avoid additional error by interpolating the gauge data into a 0.25° gridded data, we directly carry out the pixel-point comparison. We first locate the corresponding pixel of satellite products for each gauge, and then extract grid rainfall values from the pixel, together with the gauge records, to generate the satellite-gauge data pairs for final evaluation. The study period extends from April 2008 to March 2012, for which we could get the up-to-date insight into the skill of the latest satellite-based products.

In order to investigate the region-dependent performance of precipitation estimates, we divide the whole Yangtze into

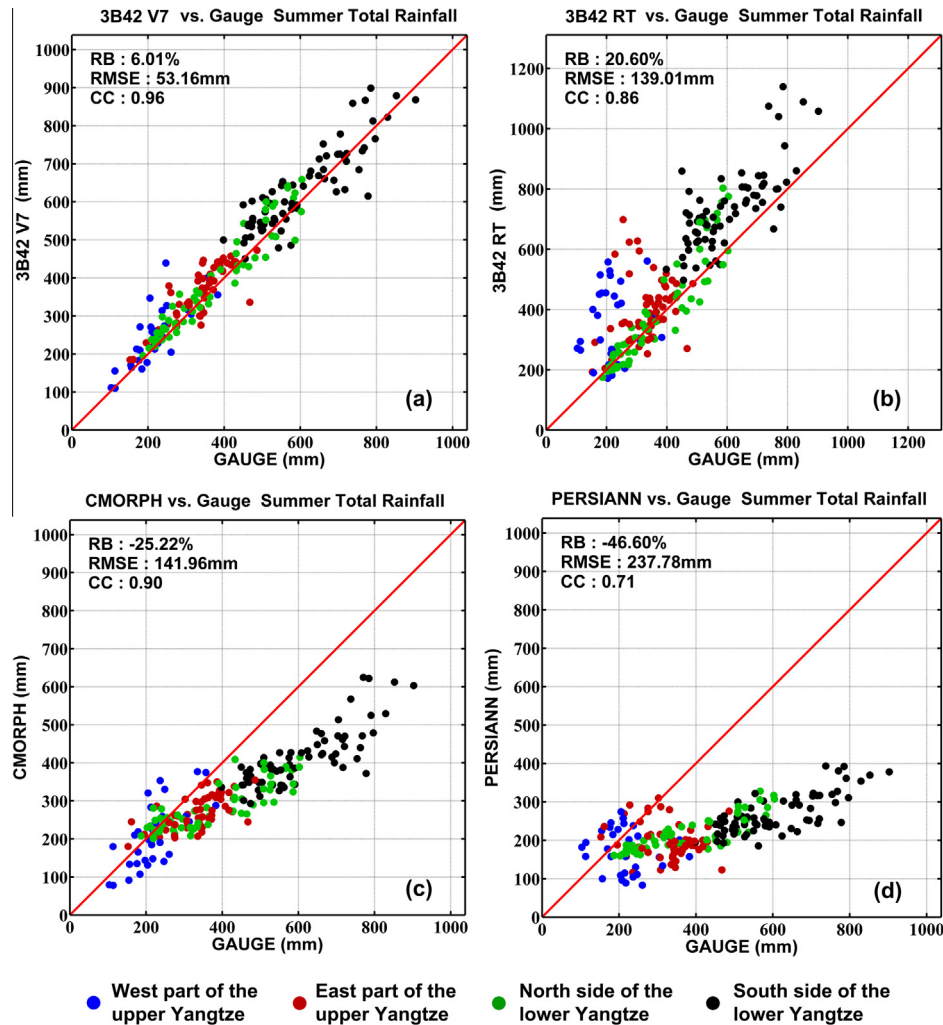


Fig. 5. Scatterplots of 4-year averaged summer accumulated precipitation (mm) at each gauge over the Yangtze River between (a) 3B42 V7 and gauge; (b) 3B42 RT and gauge; (c) CMORPH and gauge; (d) PERSIANN and gauge. Regional information was indicated by the color of dots. (For interpretation of the references to colour in this figure legend, the reader is referred to the web version of this article.)

geographical sub-regions using two rules: (1) climatic zones (National Meteorological Center, 1998) and (2) the upper, middle and lower Yangtze used in hydrology. This results in four total sub-regions (Fig. 1): (1) the western part of the upper Yangtze River, including the Chin-Sha River, which is mainly located in the Tibetan Plateau; (2) the eastern part of the upper Yangtze River, including the Min River, the Tuo River, the Wu River and the Three Gorges Region; (3) the northern side of the lower Yangtze River, including the Han River and the lower main stream; and (4) the southern side of the lower Yangtze River, including the river systems of Dongting Lake and Poyang Lake.

To understand the seasonal pattern of satellite estimated errors, we partition each year into four seasons. Contrary to typical seasons used in climatology, we define the spring as January–March (JFM), the summer as April–June (AMJ), the autumn as July–September (JAS), and the winter as October–December (OND). Such a classification method is consistent with the flood season (AMJ and JAS) at Yangtze and is thus useful for studying the hydrological cycle in this region.

To assess the performance of high-resolution satellite-based precipitation products on the daily scale, we integrate the original three-hourly precipitation estimates into daily records for each satellite dataset. Then for longer temporal (annual and seasonal) comparisons, the daily records both from satellites and gauges are accumulated.

Yangtze River precipitation is strongly affected by the East Asian monsoon, which is characterized by great inter-annual variability as well as precipitation amounts concentrated during the flood season in the form of storms. Therefore we will discuss the performance of satellite-based precipitation products in terms of these features: inter-annual variability, seasonal variability, and high-intensity precipitation events, which represent the annual, seasonal and daily scale analyses, respectively.

3. Results and discussions

In this section of the study, we discuss the performance of the four satellite products over different time scales, using several statistical metrics (Ebert et al., 2007; Tian et al., 2010) including bias, Root Mean Square Error (RMSE), spatial and temporal correlation, Probability of Detection (POD), probability distribution functions (PDFs) and others.

3.1. Detection of annual precipitation pattern and inter-annual variability

We start with the evaluation of 4-year averaged accumulated annual precipitation (mm day^{-1}) for each gauge over the Yangtze River basin. Fig. 2 shows the spatial distribution of mean bias for

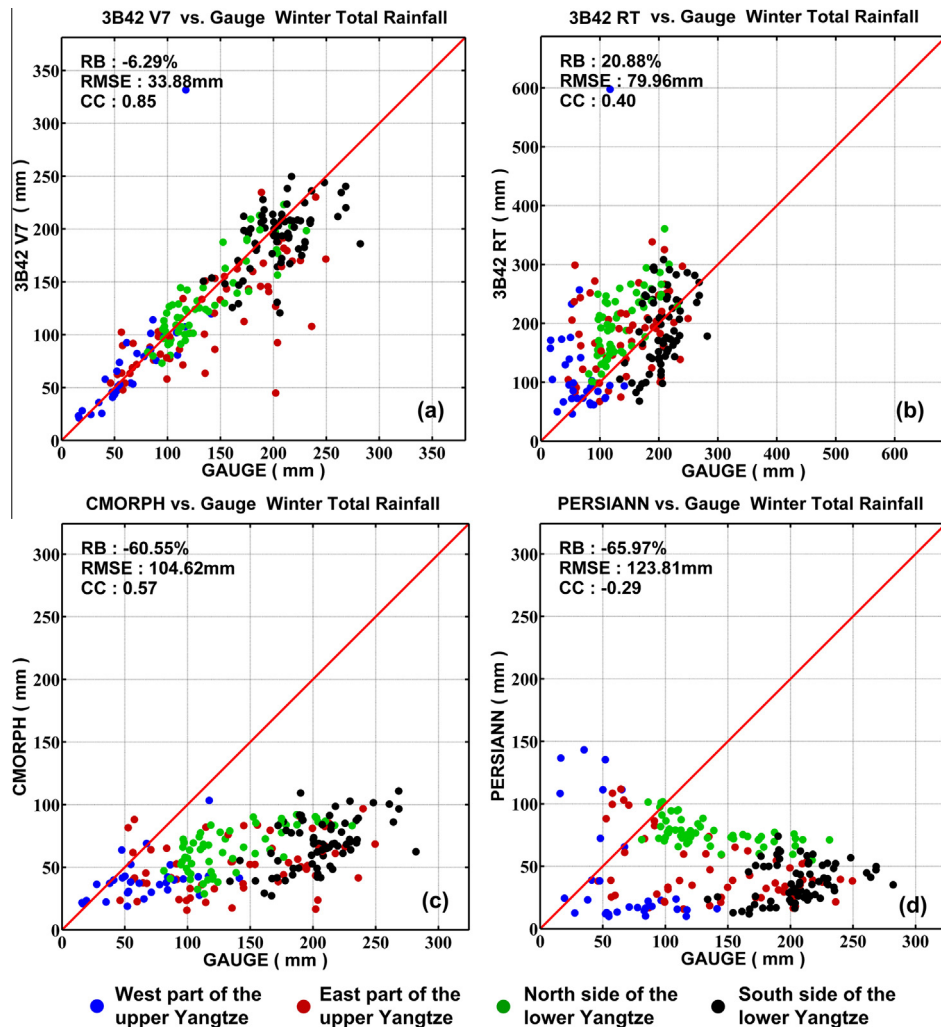


Fig. 6. The same as Fig. 5 but for 4-year averaged winter accumulated precipitation.

accumulated annual precipitation between the different satellite products estimates and gauge records. It is clear that 3B42 V7 is in the closest agreement with the CDGCD-V3; overall, the low bias of 3B42 V7 is attributed to the critical role of ground gauges in the bias removal process. Comparatively, the satellite estimates without gauge adjustment, such as 3B42 RT, CMORPH, and PERSIANN have evident local bias over the whole region.

Fig. 2 also shows that the PMW-calibrated IR techniques (3B42 RT and PERSIANN) overestimate (by $>1 \text{ mm day}^{-1}$ and $0.5\text{--}1 \text{ mm day}^{-1}$, respectively) precipitation in the upper Yangtze over the Tibetan Plateau. This bias is mostly caused by the PMW-based estimates (Shen et al., 2010), so we suspect that this kind of error is introduced by ice or snow cover, which tends to complicate PMW-based retrievals over the land surface (Tian et al., 2007). Another potential problem at the upper Yangtze is the density of gauge network; sparse gauge observations cannot provide sufficient ground reference values. Because it uses a different type of retrieval algorithm, CMORPH seems to underestimate precipitation (by -0.2 to -1 mm day^{-1}) in this region, though it slightly overestimates precipitation in a few areas. This pattern is consistent with previously reported results (Shen et al., 2010; Gao and Liu, 2012). When focusing on the middle and lower Yangtze River, both CMORPH and PERSIANN underestimate ($<-1 \text{ mm day}^{-1}$) precipitation while 3B42 RT presents a mixed pattern containing both positive and negative bias. This result indicates that for hydrological

applications of these satellite products in the upper Yangtze, ground observations are a necessity; for the lower parts of the Yangtze, 3B42 RT may be the best ‘uncalibrated’ dataset for annual scale hydrological analysis in the context of bias. With no consideration of timeliness, 3B42 V7 is the most appropriate candidate for long-term regional water budget studies.

To investigate the inter-annual variability of annual precipitation, we also analyze the performance of each product for each individual year (Table 1). This analysis indicates that each of the four products performs consistently during the four-year period, in which 2010 is a wet year and 2009 is a dry year. 3B42 V7 stably shows the lowest relative bias, and for the ‘uncalibrated’ real-time datasets, 3B42 RT always overestimates while both CMORPH and PERSIANN tend to underestimate. The general conclusions of the annual scale analyses discussed above still hold when looking at individual years from 2008 to 2012.

3.2. Detection of seasonal precipitation and its variability

Seasonal variation in the error characteristics of the precipitation estimates will provide insights into the potential factors that impact estimate accuracy in a way that varies through time. The Yangtze River is greatly impacted by frequent floods during summer and by frequent local droughts in winter, so we pay special attention to how performance varies from season to season.

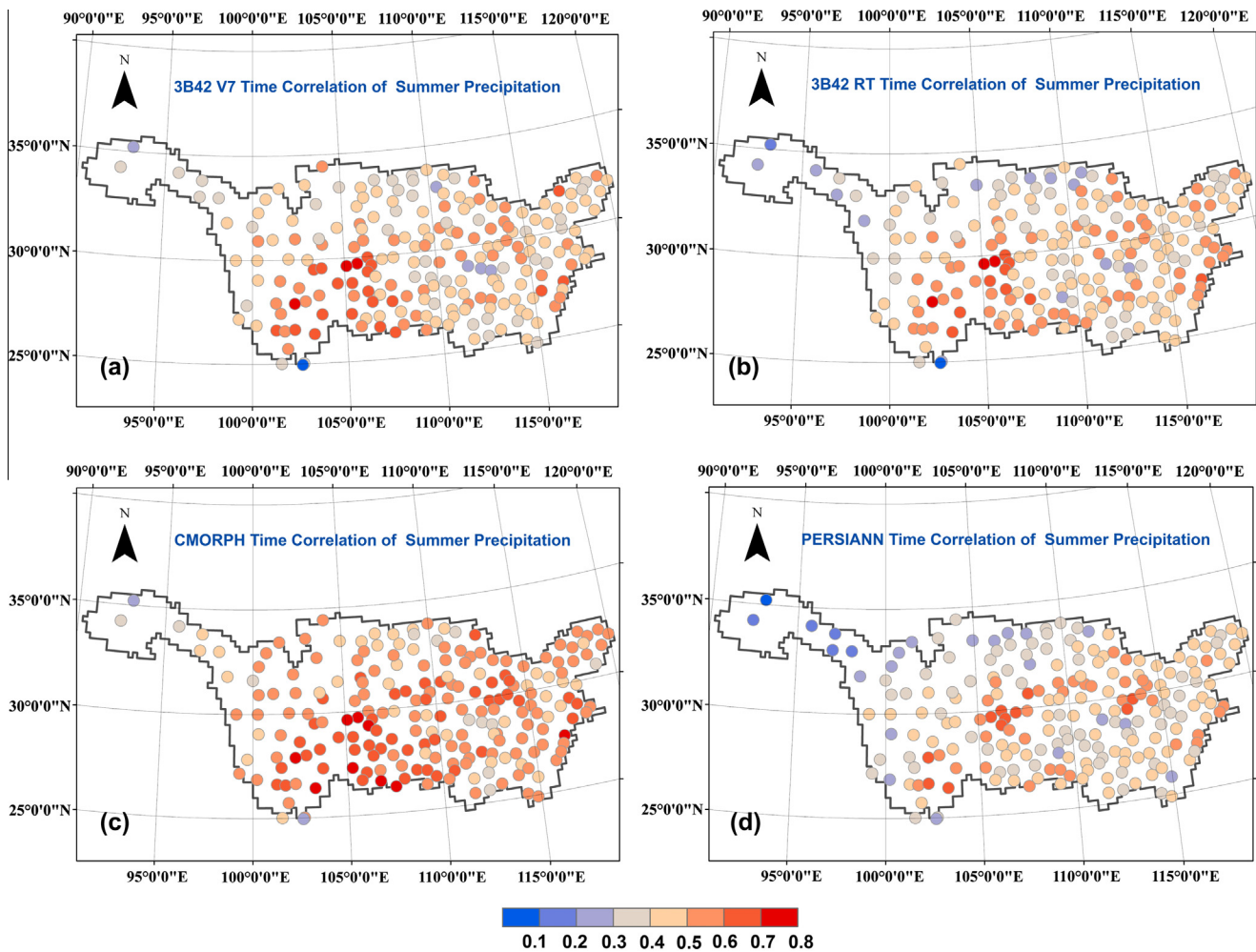


Fig. 7. Time correlation of daily precipitation in summer at each gauge over the Yangtze River between (a) 3B42 V7 and gauge; (b) 3B42 RT and gauge; (c) CMORPH and gauge; (d) PERSIANN and gauge.

Here we group the four seasons into two categories: the warm period (summer and autumn, also called the flood season) and the cold period (winter and spring). Figs. 3 and 4 show the spatial map of seasonal relative bias for the warm period and the cold period, respectively. Because gauge adjustment reduces the bias greatly, the results of 3B42 V7 are ignored here. This allows us to focus on the near real-time products, which are useful for operational hydrological prediction.

In the warm period (Fig. 3), PERSIANN performs the worst of the three estimates, with great underestimation (by -80% to -20%) while CMORPH shows slight underestimation (by -50% to 20%) over the middle and lower Yangtze. 3B42 RT captures the summer precipitation pattern for most region with small relative bias in either direction (-20% to 50%). But in the cold period (Fig. 4), it is clear that the performance declines for all three products: PERSIANN and CMORPH seriously underestimated precipitation (by -50% or more) over most regions, and the spatial pattern of 3B42 RT also becomes more complicated (though the magnitude of bias is smaller than that of the other products). As droughts have often occurred in the Yangtze River during recent years, significantly, this underestimated winter and spring precipitation makes drought monitoring and prediction difficult.

Additionally, we separate out the contribution of each season to the total bias in an annual scale analysis. For 3B42 RT, there is a long-lasting and serious overestimation of precipitation at the upper Yangtze River during all seasons (Figs. 3a and b and 4a

and b). CMORPH suffers from season-dependent biases at some places in the upper Yangtze (such as the source area of the Yangtze), with underestimation during the warm period (Fig. 3c and d) and overestimation in the cold period (Fig. 4c and d). For the lower parts of Yangtze, we found CMORPH underestimation on the annual scale mainly results from the cold season (Fig. 4c and d). As we inferred, this seasonal 'shift' in CMORPH performance may be related to the PMW measurement method, which yields better retrievals with strong convective precipitation in summer (Tian et al., 2007). The pattern of PERSIANN is very complicated and always the worst during all seasons; we suspect this can be explained by the lack of training of the artificial neural network parameters over China since PERSIANN is only adequately trained over the United States.

We also note that all three datasets do the worst during the winter when compared to other seasons (OND; Fig. 4a, c and e) and show strange 'stratified' bias patterns which extend in the north-south direction. This conflicts strongly with the actual precipitation pattern during this season (figures not shown here), which gradually increases from the west to the east. We speculate that this is due to the issue of path overlapping between different satellites in this region, but this is a question that should be answered in future research.

Similarly, Figs. 5 and 6 show the results of different products when estimating summer and winter precipitation. Generally, all datasets perform better in summer with smaller relative bias

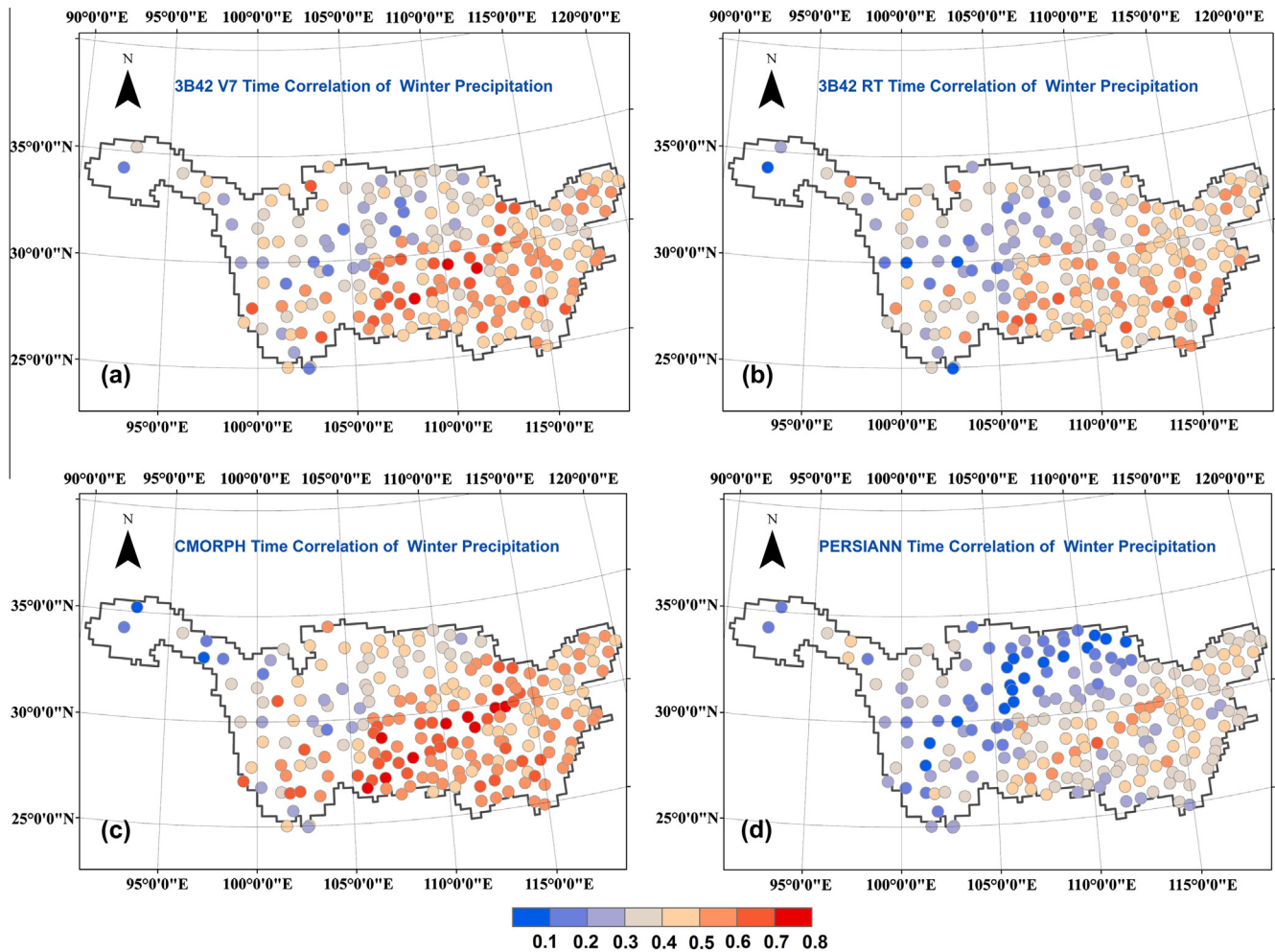


Fig. 8. The same as Fig. 7 but of daily precipitation in winter.

(RB) and higher correlation coefficient (CC). With ground gauge adjustment included, all statistics related to 3B42 V7 show significant superiority over the other products during both summer and winter. Comparing those unadjusted datasets (i.e., not 3B42 V7), we find that CMORPH exhibits the best correlation with gauge observations. This result suggests that the accuracy of the CMORPH estimates could be improved substantially if gauge information was provided to remove the bias.

At the same time, these scatterplots also provide insights into the relationship between the seasonal precipitation bias and rain rate. For CMORPH, it is evident that the bias is strongly dependent on rain rate during both summer (Fig. 5c) and winter (Fig. 6c). As the rain rate increases from the upper to the lower Yangtze, the biases also increase, almost linearly. Other research has claimed that the CMORPH bias shows strong dependence on the surface rainfall rate (Habib et al., 2012). However, the results of the 3B42 RT and PERSIANN analyses show a much more scattered pattern without this dependence on rain rate, especially in winter. Finally, we separate the gauge-satellite data pairs from different sub-regions and display them using different colors in Figs. 5 and 6. Taking this into account, we find that the lower parts of the Yangtze always get better-correlated estimates from the satellite estimates.

Thus, in flood season, all these products are expected to perform better than during dry or drought seasons. CMORPH is of great potential use during the summer. It is useful when coping with water resources management problems, such as irrigation and water supply, but we should be careful when applying this data to lower

parts of the Yangtze where precipitation amounts are greater, since the bias in the product is amplified for greater rainfall amounts.

3.3. Detection of daily dynamics and high-intensity rainfall

As the main input to operational hydrological simulations, daily precipitation is of critical importance, and accurate daily precipitation estimates help to capture watershed dynamic responses, especially for flooding processes.

First, we calculate time correlation of daily precipitation at each gauge in the Yangtze region for both summer (Fig. 7) and winter (Fig. 8). Correlation is greater than 0.4 over most gauges of the Yangtze for all the datasets, but shows degradation from summer to winter. There is a clear spatial pattern of gradual increase in correlation from the west to the east, and the extent of low-correlation region expands eastward during winter. CMORPH shows the largest correlation values during both summer (most are larger than 0.5) and winter (most are larger than 0.4), and remarkably, gets even better results than the gauge-adjusted 3B42 V7 product.

Fig. 9 shows the temporal variations of some basin-scale averaged spatial statistics computed from pixel-gauge pairs of daily precipitation. These statistics include bias, spatial correlation, RMSE and POD. To filter out high-frequency noise, we use a 30-day moving window to generate a smoothed time series. All the time series present a sort of periodic oscillation related to the seasonal variation mentioned above. The bias (Fig. 9a) results indicate that CMORPH and PERSIANN always underestimate the regional

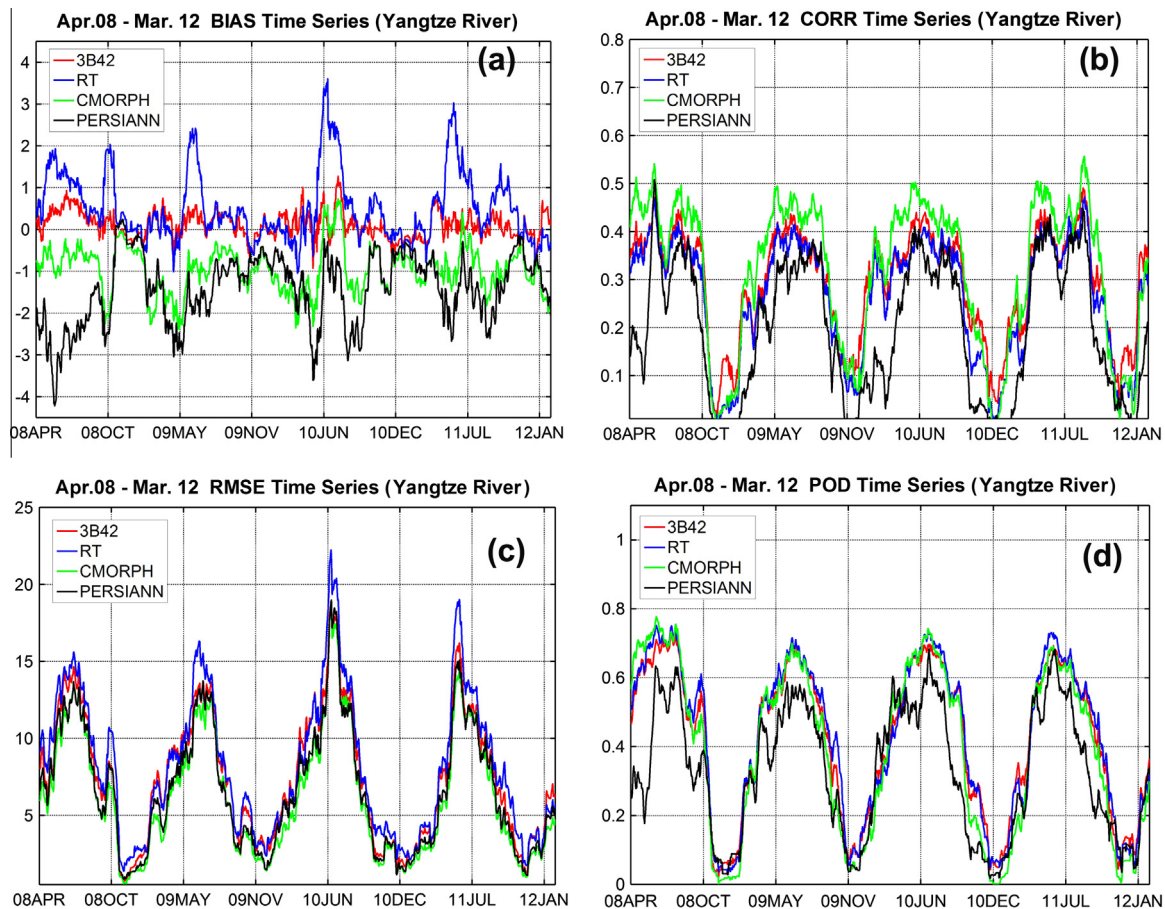


Fig. 9. Daily time series of basin-scale averaged skill measures of satellite products: (a) bias (mm day^{-1}); (b) spatial correlation; (c) RMSE; and (d) POD. A 30-day running average was applied to each time series to filter out the high-frequency noise.

mean value while 3B42 RT always overestimates it. Also we can see that 3B42 RT often shows some sharp peaks (up to 3.5 mm day^{-1}) during the warm period, and this pulse-like amplification of rainfall amount would likely introduce unrealistic flood peaks during the summer. In the spatial correlation (Fig. 9b) and RMSE (Fig. 9c) analyses, CMORPH still performs similarly to or slightly better than 3B42 V7. This result, combined with the POD (Fig. 9d) analysis, suggests that CMORPH performs better in the context of detecting daily precipitation dynamics, at least during the summer.

There are many other occurrence statistics of daily precipitation estimates for different satellite precipitation products in Fig. 10. The frequency bias (FBIAS) measures whether the rain was estimated too often or too infrequently. The equitable threat score (ETS) quantifies how well the occurrence of rain was detected, while the POD and False Alarm Ratio (FAR) clarify the nature of the occurrence errors (Ebert et al., 2007). During the summer, the mean value of FBIAS (Fig. 10a) for TMPA series, CMORPH and PERSIANN is about 1.5, which indicates that all products estimate rainfall more frequently than gauge measurements do. In winter, this value gets to be diverse while POD decreases significantly (Fig. 10b) and FAR increases (Fig. 10c). This implies that satellites do not currently capture winter precipitation correctly and induce lots of false alarms. In general, the highest ETS score (Fig. 10d) is only around 0.2, far below 1.0, which would be a perfect score, for TMPA series and CMORPH during the summer time over the Yangtze.

The results here indicate that CMORPH has the ability to detect rainfall events and to capture large-scale rainfall spatial

distribution, both of which impact basin-scale flood generation and propagation. We again suggest that there is a high potential for using this data in watershed flood prediction.

Probability distribution functions (PDFs) can provide us with detailed information on the frequency of rainfall with different intensities; this is important since the same rainfall amount in the form of long-lasting light rain or a short duration storm will yield quite different flood patterns. As a consequence, the occurrence PDF (PDFc) and precipitation volume PDF (PDFv) estimated from each satellite product and gauge data are compared. The PDFc is computed as a ratio between the number of times precipitation occurs inside each bin (as in a histogram) and the total number of times precipitation occurs overall. The PDFv is computed as a ratio between the sum of the precipitation rates inside each bin and the total sum of precipitation rates (Kirstetter et al., 2012). Here, only pixel-gauge pairs which both ground reference and satellite precipitation estimates are nonzero can be selected to compute the PDFc and PDFv.

In summer (Fig. 11a), CMORPH and PERSIANN miss some precipitation events where the rain rate is greater than 16 mm day^{-1} , and tend to detect more cases than are observed by gauges when rain rates fall below 16 mm day^{-1} . In comparison, 3B42 RT underestimates the occurrence frequency when low rain rates ($<2 \text{ mm day}^{-1}$) are occurring and evidently overestimates the occurrence frequency when the 8 mm day^{-1} threshold is exceeded. In winter (Fig. 11b), the performance of all products declines but the general pattern is similar to that seen in the summer analyses.

The volume PDF estimates shows the rain intensity distribution of daily precipitation amount. This information has great

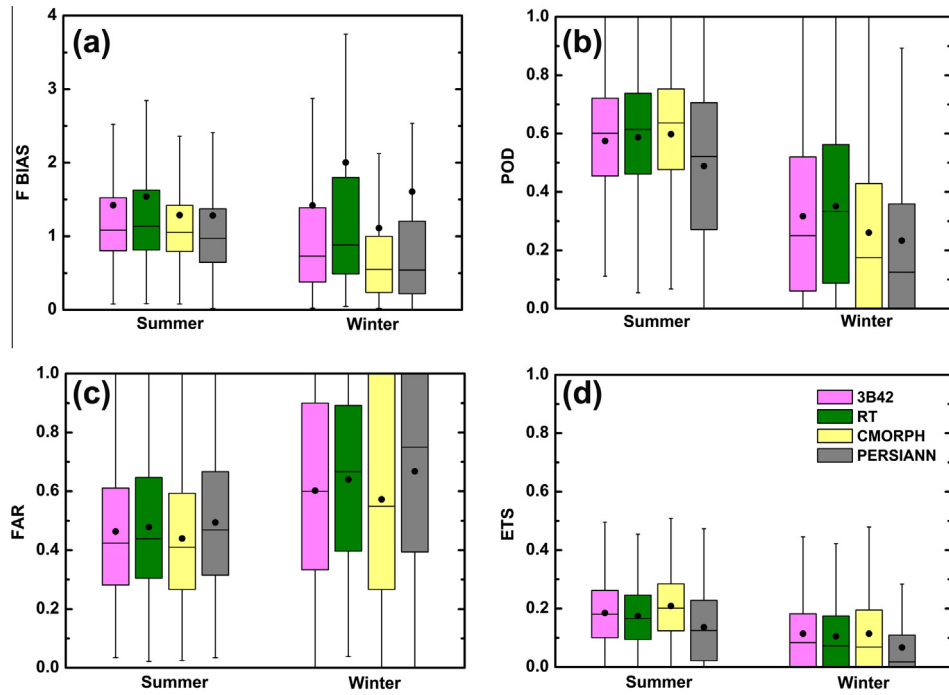


Fig. 10. The boxplots of daily values of (a) F BIAS, (b) POD, (c) FAR, and (d) ETS in summer and winter. These are evaluation metrics of the estimated occurrence for precipitation exceeding the threshold of 1 mm day^{-1} over the Yangtze River. (The dot represents the mean value. Each box ranges from the lower 25th q quartile to the upper 75th quartile. The median is presented by the middle line in the box. The whiskers extend out to largest and smallest values.)

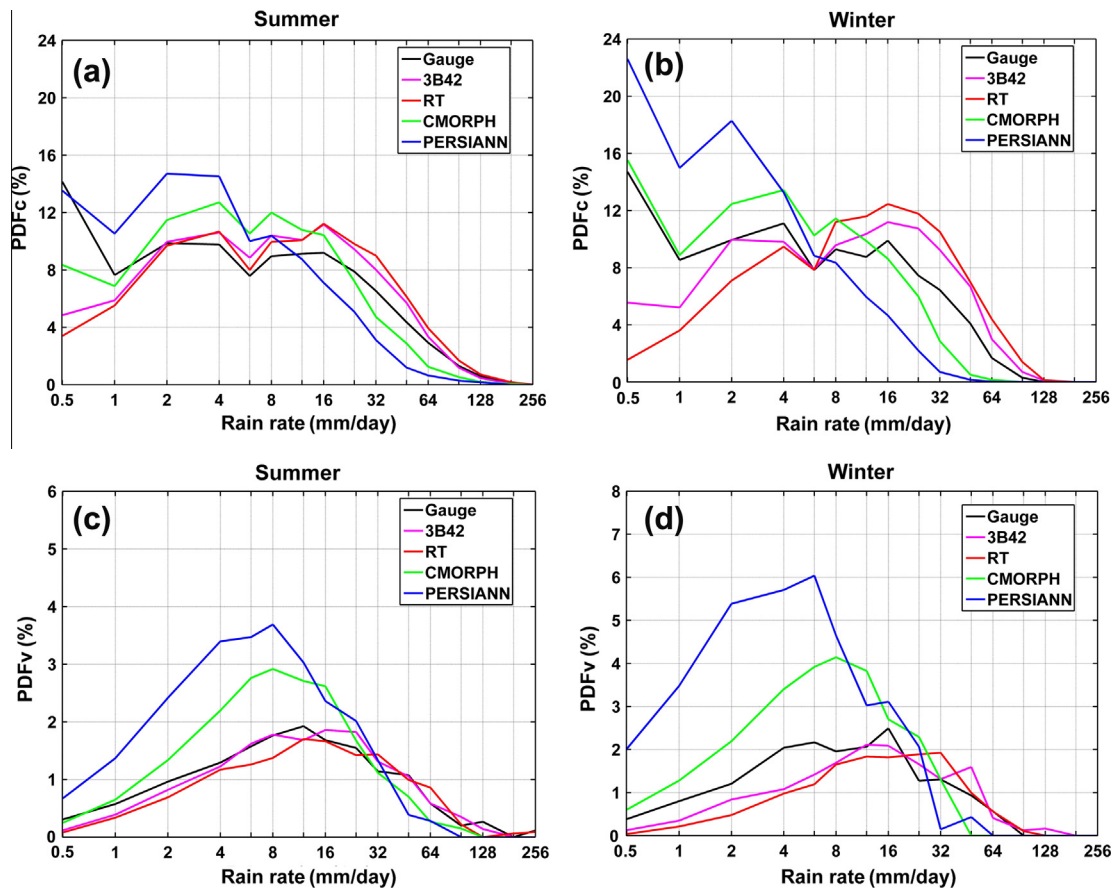


Fig. 11. The occurrence probability distribution functions (PDFc; left) and volume probability distribution functions (PDFv; right) of precipitation estimates in summer and winter. (The PDFs are calculated based on pixel-gauge pairs in which both ground precipitation and satellite precipitation estimates are nonzero.)

significance for hydrological simulation since most hydrological processes, like surface runoff, are highly sensitive to rainfall intensity distributions as well as the total amount of rainfall (Tian et al., 2010). During summer time (Fig. 11c), CMORPH and PERSIANN considerably overestimate precipitation volume when rain rates lower than 32 mm day^{-1} are occurring, but they slightly underestimate precipitation volume when rainfall are greater than that threshold. TMPA products show better agreement with the PDFv of gauge records, in both summer and winter.

According to this PDFs-based analysis, we see that for local floods generated by high-intensity rainfall in the Yangtze, TMPA series data perform the best. However, this inference should be examined carefully in future work especially for hydrological applications.

4. Conclusions

High-resolution multi-sensor blended global precipitation products have significantly improved our ability to monitor large-scale precipitation dynamics during the past decades. In this study, we evaluated and compared four sets of the state-of-the-art satellite-based precipitation products, 3B42 V7, 3B42 RT, CMORPH, and PERSIANN, over the Yangtze region – the largest river basin in China. Using the gauge data as the ground reference, we investigated the quality of different precipitation products across multiple time scales with a regional focus, including the spatial pattern and temporal variation of error characteristics associated with these satellite products. The main findings can be summarized as follows:

- (1) Compared over the entire Yangtze River basin at different temporal scales, in general, 3B42 RT (CMORPH) overestimates (underestimates) precipitation while 3B42V7 (PERSIANN) shows least (most) bias. Spatially, the upper Yangtze suffers more severe systematic errors for all datasets.
- (2) There are apparent precipitation regime-dependent errors that also relate to the seasons. All the products demonstrate better performance in the warm period. In the upper Yangtze River, there is a yearlong systematic overestimation for 3B42 RT, while CMORPH suffers from underestimation during the warm period and overestimation in the cold period. In the lower Yangtze, the results indicate the underestimation of CMORPH mainly occurs during the cold season.
- (3) Considering spatial and temporal correlations, RMSE, POD and other occurrence statistics, CMORPH consistently shows good skill among the near-real-time products during the summer. However, the bias of CMORPH shows strong linear dependence on the surface rain rate during both summer and winter, and exhibits greater bias in high rainfall intensity.
- (4) Gauge adjustment in 3B42 V7 greatly reduces the bias from daily to annual totals, and also helps to keep the skill levels stable during the winter. However, 3B42 V7 does not always show superiority over other products, in particular CMORPH, when the spatial correlation, RMSE, and POD are considered for daily comparison.
- (5) Finally the PDFs-based investigation indicates that the PDFs of TMPA series datasets (3B42 V7 and 3B42 RT) are much closer to that observed by the gauges, especially when high-intensity rain rates are being considered.

These results indicate that each individual satellite rainfall product has its own pros and cons in the context of various hydrological applications. 3B42 V7 is probably the most appropriate dataset for long-term regional water balance studies. For basin-wide

large-scale flood prediction, CMORPH seems to be able to provide better detection and spatial variability, but caution is warranted when applying CMORPH to the lower Yangtze where its bias will be amplified due to high rainfall intensity there. Finally, for small-scale floods or flash floods induced by localized high-intensity rainfall events, the TMPA series dataset will likely perform better.

Due to the complicated precipitation pattern itself over the Yangtze River affected by both monsoon climate and complex terrains, the results reported here just reveal preliminary answers to the critical questions of characterizing the errors of various precipitation estimates, understanding their causes, and improving accuracy of satellite precipitation estimates in this both socioeconomically and ecologically important region. This kind of evaluation should be continued and, more desirably, implemented in an operational mode with a range of regional hydrological applications. Based on this study, we would like to further address some other critical issues: (1) evaluation of diurnal variability using satellite precipitation products, a critical factor for flash floods during storm season; (2) application of remote sensing precipitation to a distributed Yangtze hydrological model to characterize the error propagation mechanisms from forcing to hydrological response; (3) synergistic development of multi-source merged precipitation products from gauges, radars, and satellites to better infer the 'true' value of regional precipitation. All these goals work together, we believe, to substantially improve the skill of hydrological prediction and natural hazards monitoring in Yangtze River basin.

Acknowledgments

This research was supported by the National Natural Science Funds for Distinguished Young Scholar (Project No. 51025931) and the National Natural Science Foundation of China (Project No. 50939004). The first author was also partially supported by Tsinghua Scholarship for Overseas Graduate Studies. The first author would like to thank the HyDROS Lab (HyDRometeorology and RemOte Sensing Laboratory: <http://hydro.ou.edu>) at the National Weather Center, Norman, OK for their support during his visiting, and also acknowledge Robert Clark for his useful comments and language editing which have greatly improved this manuscript. The authors wish to thank Dr. Bellie Sivakumar and other two anonymous reviewers for their valuable comments.

References

- Aragão, L.E.O.C., Malhi, Y., Roman-Cuesta, R.M., Saatchi, S., Anderson, L.O., Shimabukuro, Y.E., 2007. Spatial patterns and fire response of recent Amazonian droughts. *Geophys. Res. Lett.* 34, L07701.
- China Meteorological Administration, 2012. National Meteorological Information Center data documentation for China Daily Ground Climate Dataset (V3.0), online is available: <http://cdc.cma.gov.cn/home.do>.
- Dinku, T., Ruiz, F., Connor, S.J., Ceccato, P., 2010. Validation and intercomparison of satellite rainfall estimates over Colombia. *J. Appl. Meteor. Climatol.* 49, 1004–1014.
- Ebert, E.E., Janowiak, J.E., Kidd, C., 2007. Comparison of near-real-time precipitation estimates from satellite observations and numerical models. *Bull. Am. Meteor. Soc.* 88, 47–64.
- Gao, Y., Liu, M., 2013. Evaluation of high-resolution satellite precipitation products using rain gauge observations over the Tibetan Plateau. *Hydrol. Earth Syst. Sci. Discuss* 9, 9503–9532.
- Gourley, J.J., Hong, Y., Flamig, Z.L., Li, L., Wang, J., 2010. Intercomparison of rainfall estimates from radar, satellite, gauge, and combinations for a season of record rainfall. *J. Appl. Meteorol. Climatol.* 49, 437–452.
- Gu, H., Yu, Z., Yang, C., Qin, J., Lu, B., Liang, C., 2010. Hydrological assessment of TRMM rainfall data over Yangtze River Basin. *Water Sci. Eng.* 3, 418–430.
- Habib, E., Haile, A., Tian, Y., Joyce, R., 2012. Evaluation of the high-resolution CMORPH satellite rainfall product using dense rain gauge observations and radar-based estimates. *J. Hydrometeorol.* 13, 1784–1798.
- Heike, H., Becker, S., Jiang, T., 2012. Precipitation variability in the Yangtze River subbasins. *Water Int.* 37, 16–31.

- Heistermann, M., Kneis, D., 2011. Benchmarking quantitative precipitation estimation by conceptual rainfall-runoff modeling. *Water Resour. Res.* 47, W06514.
- Hirpa, F.A., Gebremichael, M., Hopson, T., 2010. Evaluation of high-resolution satellite precipitation products over very complex terrain in Ethiopia. *J. Appl. Meteor. Climatol.* 49, 1044–1051.
- Hong, Y., Hsu, K.L., Gao, X., Sorooshian, S., 2004. Precipitation estimation from remotely sensed imagery using artificial neural network-cloud classification system (PERSIANN-CCS). *J. Appl. Meteor. Climatol.* 43, 1834–1853.
- Hong, Y., Adler, R.F., Huffman, G.J., 2006. Evaluation of the potential of NASA multi-satellite precipitation analysis in global landslide hazard assessment. *Geophys. Res. Lett.* 33, L22402.
- Hossain, F., Lettenmaier, D.P., 2006. Flood prediction in the future: recognizing hydrologic issues in anticipation of the Global Precipitation Measurement mission. *Water Resour. Res.* 42, W11301.
- Huffman, G.J., Adler, R.F., Morrissey, M., Bolvin, D.T., Curtis, S., Joyce, S., McGavock, B., Susskind, J., 2001. Global precipitation at one-degree daily resolution from multisatellite observations. *J. Hydrometeorol.* 2, 36–50.
- Huffman, G.J., Adler, R.F., Bolvin, D.T., Gu, G., Nelkin, E.J., Bowman, K.P., Hong, Y., Stocker, E.F., Wolff, D.B., 2007. The TRMM multi-satellite precipitation analysis (TMPA): quasi-global, multi-year, combined-sensor precipitation estimates at fine scales. *J. Hydrometeorol.* 8, 38–55.
- Huffman, G.J., Bolvin, D.T., Nelkin, E.J., Adler, R.F., 2011. Highlights of version 7 TRMM multi-satellite precipitation analysis (TMPA). In: Klepp, C., Huffman, G.J., (Eds.), 5th Internat. Precip. Working Group Workshop, Workshop Program and Proceedings, 11–15 October 2010, Hamburg, Germany. Reports on Earth Sys. Sci., 100/2011, Max-Planck-Institut für Meteorologie, pp. 109–110.
- Jiang, S., Ren, L.-L., Hong, Y., Yong, B., Yang, X., Yuan, F., Ma, M., 2012. Comprehensive evaluation of multi-satellite precipitation products with a dense rain gauge network and optimally merging their simulated hydrological flows using the Bayesian model averaging method. *J. Hydrol.* 452–453, 213–225.
- Joyce, R.J., Janowiak, J.E., Arkin, P.A., Xie, P., 2004. CMORPH: a method that produces global precipitation estimates from passive microwave and infrared data at high spatial and temporal resolution. *J. Hydrometeorol.* 5, 487–503.
- Kirstetter, P.-E., Hong, Y., Gourley, J.J., Chen, S., Flamig, Z., Zhang, J., Schwaller, M., Petersen, W., Amitai, E., 2012. Toward a framework for systematic error modeling of spaceborne precipitation radar with NOAA/NSSL ground radar-based national mosaic QPE. *J. Hydrometeorol.* 13, 1285–1300.
- Kubota, T., Shige, S., Hashizume, H., Aonashi, K., Takahashi, N., Seto, S., Takayabu, Y.N., Ushio, T., Nakagawa, K., Iwanami, K., Kachi, M., Okamoto, K., 2007. Global precipitation map using satellite-borne microwave radiometers by the GSMaP Project: production and validation. *IEEE Trans. Geosci. Remote Sens.* 45, 2259–2275.
- Li, X., Zhang, Q., Xu, C., 2012. Suitability of the TRMM satellite rainfalls in driving a distributed hydrological model for water balance computations in Xinjiang catchment, Poyang lake basin. *J. Hydrol.* 426–427, 28–38.
- Mishra, A.K., Coulibaly, P., 2009. Developments in hydrometric network design: a review. *Rev. Geophys.* 47, RG2001.
- National Meteorological Center, 1998. Names and codes for climate regionalization in China—Climatic zones and climatic regions. GB/T 17297-1998.
- Nijssen, B., Lettenmaier, D.P., 2004. Effect of precipitation sampling error on simulated hydrological fluxes and states: anticipating the global precipitation measurement satellites. *J. Geophys. Res.* 109, D02103.
- Shen, Y., Xiong, A., Wang, Y., Xie, P., 2010. Performance of high-resolution satellite precipitation products over China. *J. Geophys. Res.* 115, D02114.
- Sohn, S.-J., Tam, C.-Y., Ashok, K., Ahn, J.-B., 2012. Quantifying the reliability of precipitation datasets for monitoring large-scale East Asian precipitation variations. *Int. J. Climatol.* 32, 1520–1526.
- Sorooshian, S., Hsu, K.L., Gao, X., Gupta, H., Imam, B., Braithwaite, D., 2000. Evaluation of PERSIANN system satellite-based estimates of tropical rainfall. *Bull. Am. Meteorol. Soc.* 81, 2035–2046.
- Sorooshian, S., AghaKouchak, A., Arkin, P., Eylander, J., Fofoula-Georgiou, E., Harmon, R., Hendrickx, J.M.H., Imam, B., Kuligowski, R., Skahill, B., Gail Skofronick-Jackson, G., 2011. Advanced concepts on remote sensing of precipitation at multiple scales. *Bull. Am. Meteor. Soc.* 92, 1353–1357.
- Su, F., Hong, Y., Lettenmaier, D.P., 2008. Evaluation of TRMM multisatellite precipitation analysis and its utility in hydrologic prediction in the La Plata Basin. *J. Hydrometeorol.* 9, 622–640.
- Tian, Y., Peters-Lidard, C.D., Choudhury, B.J., Garcia, M., 2007. Multitemporal analysis of TRMM-based satellite precipitation products for land data assimilation applications. *J. Hydrometeorol.* 8, 1165–1183.
- Tian, Y., Peters-Lidard, C.D., Adler, R.F., Kubota, T., Ushio, T., 2010. Evaluation of GSMaP precipitation estimates over the contiguous United States. *J. Hydrometeorol.* 11, 566–574.
- Turk, F.J., Miller, S.D., 2005. Toward improving estimates of remotely sensed precipitation with MODIS/AMSR-E blended data techniques. *IEEE Trans. Geosci. Remote Sens.* 43, 1059–1069.
- Turk, F.J., Arkin, P., Sapiano, M.R.P., Ebert, E.E., 2008. Evaluating high-resolution precipitation products. *Bull. Am. Meteor. Soc.* 89, 1911–1916.
- Wu, H., Adler, R.F., Hong, Y., Tian, Y., Policelli, F., 2012. Evaluation of global flood detection using satellite-based rainfall and a hydrologic model. *J. Hydrometeorol.* 13, 1268–1284.
- Yin, Z.-Y., Zhang, X., Liu, X., Colella, M., Chen, X., 2008. An assessment of the biases of satellite rainfall estimates over the Tibetan Plateau and correction methods based on topographic analysis. *J. Hydrometeorol.* 9, 301–326.
- Yong, B., Hong, Y., Ren, L.-L., Gourley, J.J., Huffman, G.J., Chen, X., Wang, W., Khan, S.I., 2012. Assessment of evolving TRMM-based multisatellite real-time precipitation estimation methods and their impacts on hydrologic prediction in a high latitude basin. *J. Geophys. Res.* 117, D09108.
- Zhang, J., Howard, K., Langston, C., Vasiloff, S., Kaney, B., Arthur, A., Cooten, S.V., Kelleher, K., Kitzmiller, D., Ding, F., Seo, D.J., Wells, E., Dempsey, C., 2011. National Mosaic and Multi-sensor QPE (NMQ) System: Description, results, and future plans. *Bull. Am. Meteor. Soc.* 92, 1321–1338.
- Zhou, T., Yu, R., Chen, H., Dai, A., Pan, Y., 2008. Summer precipitation frequency, intensity, and diurnal cycle over China: a comparison of satellite data with rain gauge observations. *J. Clim.* 21, 3997–4010.